Journal of Chromatography, 142 (1977) 61–86

CHROM. 10,320

EXPERIMENTAL CHARACTERIZATION OF ELUTION PROFILES IN GAS CHROMATOGRAPHY USING CENTRAL STATISTICAL MOMENTS

STUDY OF THE RELATIONSHIP BETWEEN THESE MOMENTS AND MASS TRANSFER KINETICS IN THE COLUMN

CLAIRE VIDAL-MADJAR and GEORGES GUIOCHON
Laboratoire de Chimie Analytique Physique, École Polytechnique, 91128 Palaiseau (France)

SUMMARY

A high-precision gas chromatograph under computer control, with digital data acquisition of the chromatographic signal, was used to measure the central statistical moments of chromatographic zones. It is shown that for fairly symmetrical peaks, the moments are determined with a better accuracy, even at a low signal-to-noise ratio, from a least-squares fit of the Gram–Charlier series on the experimental elution profiles.

The Gram–Charlier series is a good model for representing the peak elution profile provided that the skew coefficient is small. The second central moment derived from the Gram–Charlier model was studied as a function of the carrier gas velocity, using the usual HETP concept. The third and the fourth central moments were found to follow similar relationships to the carrier gas velocity.

For strongly tailing peaks, it is shown that the moments are not sufficient for characterizing the peak shape. This tailing has a kinetic origin and results from slow mass transfer in the stationary phase. The time constant of the exponential decay adjusted on the peak tail gives a good indication of the desorption time of the molecule from the most active sites of the packing.

INTRODUCTION

The characterization of chromatographic peak profiles is of fundamental importance, as these profiles contain all of the information available regarding the contributions to band broadening that occur either in the column or in the instrument itself.

For the sake of simplicity in further theoretical calculations, most chromatographic theories assume that the chromatographic peak profile is gaussian[1]. Significant errors might occur, however, from this approximation as chromatographic elution curves are generally non-symmetrical.

Giddings and Eyring[2] and McQuarrie[3] derived exact expressions for the elution curve for various types of chromatographic systems, such as a column packed with

a stationary phase containing several types of retention sites and a column in which a pure retention mechanism takes place, with one type of site but with various input distributions.

McQuarrie[3] introduced a computation procedure using central statistical moments to characterize the probability density curves. The theoretical importance of these moments is now well established[4–6].

Digital acquisition of chromatographic data by a computer permits the rapid and easy calculation of the moments of the peak profile by direct integration. This procedure, however, can lead to large errors and Chesler and Cram[7] studied in detail the influence of the data acquisition and integration parameters on the precision of the moments and especially the effect of the limits of integration and the density of data points. A procedure for improving the precision of the determination of the moments of non-symmetrical signals has been discussed by Petitclerc and Guiochon[8]. An exponential decay is adjusted by numerical computation on the tail of the peak and the numerical integration is replaced with the exact contribution derived from the parameters of the exponential.

Characterization of peak shapes can thus be obtained either from the determination of central statistical moments or by fitting to the experimental data theoretical models such as the Gram–Charlier series[3] or the Poisson law[9] for the more symmetrical curves. For strongly tailing peaks when the adsorption is linear, a good model of the chromatographic profile might be that described by Giddings[10], who assumed two types of sites. Another attractive model has been suggested by Villermaux[11], which also assumes two different types of retention sites in the mass balance equation but the peak profile is derived by numerical inversion of the Laplace transform using the fast Fourier method.

In this work, we discuss whether the Giddings model for tailing peaks and the Gram–Charlier series for more symmetrical peaks are good models for accounting for the peak profile. We also compare the moments obtained by numerical integration with those calculated from the parameters of the best Gram–Charlier series obtained by fitting of the series to the digitalized chromatographic data collected by the computer. Until now, only an empirical model has been used to characterize peak shapes[12]. If possible, the use of theoretically sound models offers a better prospect as some direct insight into the mechanism of band broadening would become possible.

EXPERIMENTAL

The chromatographic equipment, specially designed for high precision measurements, has been described previously[13].

The column is kept in an oil-bath, the temperature of which is controlled to within 0.01° over a few days with a Melabs proportional controller. The inlet pressure is controlled with a Texas Instruments pressure controller working with reference to the outlet pressure, with fluctuations smaller than 0.015 mbar. The outlet pressure is controlled with a Negretti and Zambra pressure regulator working by reference to vacuum, with fluctuations smaller than 0.2 mbar.

A Carlo Erba sampling valve is used to inject 2-μl gaseous samples of a mixture of methane and the vapour of the compound being studied, diluted in the carrier gas.

A home-made flame-ionization detector is used. The signal is measured using a Keithley amplifier and a Solartron digital voltmeter (LM 1480-3, Schlumberger). The data are stored on the disk of a Hewlett-Packard 2116 B, 8K core memory. The same computer calculates the different moments of the chromatographic elution peak by numerical integration, once the data acquisition is completed and stored in the disk.

The baseline is calculated by adjusting a straight line on the chromatogram before and after the peak has been completely eluted[8], then the elution profile is corrected by subtracting this straight-line contribution. For the most strongly tailing peaks, in order to obtain a better precision for the numerical integration[8] an exponential is adjusted on the tail of the peak from a level corresponding to 2% of the maximum peak height.

A non-linear least-squares fit of the theoretical models (Gram–Charlier series, two types of sites model) was carried out on an IBM 370/168 at the Centre Inter-Regional de Calcul Electronique, Orsay, France. For this procedure, the digitalized data of the chromatogram were collected on magnetic tape.

The columns used were 2 m × 2.1 mm I.D. The first column was packed with 20% squalane on Chromosorb P AW DMCS (125–160 μm). On this column almost symmetrical peaks are obtained for alkanes, while strongly tailing peaks are observed with polar compounds such as methylene chloride and diethyl ether. On the second column, packed with 0.5% squalane on porous glass beads, DMCS (125–160 μm), (Corning, Corning, N.Y., U.S.A.), sharp peaks but with a long tailing edge were observed for alkanes.

The solutes studied were of ultra-high purity. This is very important as the moments obtained by numerical integration are completely erroneous if a small impurity eluted close to the main peak interferes with the profile of the compound to be studied. *n*-Pentane and cyclohexane (99.99% purity by gas chromatography on capillary columns) were purchased from Elf (Paris, France) and methane (> 99.995% purity, with ethane content < 15 vpm) from Air Liquide (Paris, France).

THEORETICAL

Giddings[10] has shown that in many instances peak tailing is of kinetic origin and can be explained by assuming that two retention mechanisms are superimposed: a fast exchange process with a moderate exchange energy accounts for the retention of most molecules, while a slow exchange process is responsible for the tailing.

Assuming an infinitely narrow energy distribution for the two types of sites, the elution profile is

$$P_1(\theta) = \left(\frac{a_1 a_2}{\theta}\right)^{1/2} e^{-a_1 - a_2\theta} I_1(\sqrt{4 a_1 a_2 \theta}) \quad (1)$$

where $\theta = t_s/t_m$, t_s is the time measured from the instant when the maximum of the undisturbed peak corresponding to the fast exchange process if it were alone would appear, t_m is the retention time of an unretained peak, $a_1 = k_a t_m$ and $a_2 = k_d t_m$, k_a and k_d are the adsorption and desorption rate constants and $I_1(X)$ is the Bessel function of an imaginary argument.

The molecules which are eluted from the column without ever being adsorbed on one of the active sites corresponding to the slow exchange process are not represented by eqn. 1 and the ideal profile contributed by them is

$$P_2(\theta) = e^{-a_1}\,\delta(\theta) \tag{2}$$

where $\delta(\theta)$ is the Dirac function corresponding to an infinitely narrow pulse at $\theta = 0$. The addition of eqns. 1 and 2 yields a concentration profile normalized to unit area. This undisturbed profile has been obtained assuming the conditions of ideal chromatography. It must be modified to account for the effective diffusion process inside the column, as described in the calculations below (Schmidt method).

The central statistical moments can be used to characterize the chromatographic peak shape when the theoretical model needed to describe the system is too complicated[3].

The moments are defined by the equations

$$m_n = \frac{1}{m_0}\int_0^\infty (t - m'_1)\, n\, f(t)\, dt \tag{3a}$$

and

$$m_0 = \int_0^\infty f(t)\, dt \tag{3b}$$

where $f(t)$ is the chromatographic profile at time t, m_0 the peak area and m'_1 the mass centre of the distribution curve. The skew of the distribution curve is usually defined as $S = m_3/m_2^{3/2}$ and the excess as $E = m_4/m_2^4$. $S = 0$ and $E = 3$ for a gaussian profile.

The moments can be used to describe the peak shape when the exact mathematical equation of the peak is not known. An approximation of the profile is given by the Gram–Charlier series[3]. This series is an expansion of the normal distribution:

$$\Phi(z) = \frac{1}{\sigma\sqrt{2\pi}} \exp(-z^2/2) \tag{4}$$

The profile is

$$f(z) = A_0\,[\Phi(z) + (A_1/1!)\,\Phi^{(1)}(z) + (A_2/2!)\,\Phi^{(2)}(z) + \ldots] \tag{5}$$

where the A_i are constant coefficients, $z = (t - m'_1)/\sigma$ and σ is the standard deviation of the gaussian profile, with $m_2 = \sigma^2$. Eqn. 5 can be written as

$$f(z) = \frac{m_0}{\sigma\sqrt{2\pi}} \cdot \exp(-z^2/2)\left[1 + \sum_{i=3}^{\infty} \frac{A_i}{i!} \cdot H_i(z)\right] \tag{6}$$

where H_i is the ith Hermite polynomial. If the series is expanded to the fourth term, we have

$$A_3 = m^3/\sigma^3 = S \tag{7a}$$

$$H_3(z) = z^3 - 3z \tag{7b}$$

$$A_4 = (m_4/\sigma^4) - 3 = E - 3 \tag{8a}$$

$$H_4(z) = z^4 - 6z^2 + 3 \tag{8b}$$

The skew and the excess of this distribution curve are $S = A_3$ and $E = A_4 + 3$.

Kucera[4] and Grubner[5] derived the four statistical moments from the mass-balance equations for gas–solid chromatography; Grushka[6] found similar expressions for the statistical moments in gas–liquid chromatography. These equations are given in Table I and have been re-calculated by us as they are written incorrectly in ref. 6. In Table I k' is the capacity factor, U the carrier gas velocity, D_s is the diffusion coefficient of the solute in the stationary phase, d_f is the thickness of the stationary film, V_s and V_m are the volumes of the stationary and mobile phase per unit column volume, respectively, and D is the dispersion coefficient which takes into account the effective diffusion process of the solute in the gaseous phase and the eddy diffusion phenomenon[1] which is a combined flow diffusive exchange.

TABLE I

MASS CENTRE AND CENTRAL STATISTICAL MOMENTS IN GAS–LIQUID CHROMATOGRAPHY*

$$m_1' = \left(\frac{L}{U} + \frac{2D}{U^2}\right)(1 + k')$$

$$m_2 = \left(\frac{2DL}{U^3} + \frac{8D^2}{U^4}\right)(1 + k')^2 + \left(\frac{2L}{U} + \frac{4D}{U^2}\right) k'\,T, \text{ with } T = \left(\frac{d_f^2}{3D_s} + \frac{V_s}{V_m k_f}\right)$$

$$m_3 = \left(\frac{12D^2L}{U^5} + \frac{64D^3}{U^6}\right)(1 + k')^3 + \left(\frac{12DL}{U^3} + \frac{48D^2}{U^4}\right) k'(1 + k')\,T$$

$$+ \left(\frac{6L}{U} + \frac{12D}{U^2}\right) k' \left(\frac{2\,d_f^4}{15D_s^2} + \frac{2\,d_f^2\,V_s}{3D_s\,V_m\,k_f} + \frac{V_s^2}{V_m^2\,k_f^2}\right)$$

$$m_4 = \left(\frac{12D^2L^2}{U^6} + \frac{216D^3L}{U^7} + \frac{960D^4}{U^8}\right)(1 + k')^4 + \left(\frac{24DL^2}{U^4} + \frac{288D^2L}{U^5} + \frac{960\,D^3}{U^6}\right) k'(1 + k')^2 T$$

$$+ \left(\frac{12L^2}{U^2} + \frac{72\,DL}{U^3} + \frac{144\,D^2}{U^4}\right) k'^2\,T^2$$

$$+ \left(\frac{48DL}{U^3} + \frac{192\,D^2}{U^4}\right) k'(1 + k') \left(\frac{2\,d_f^4}{15D_s^2} + \frac{2\,d_f^2\,V_s}{3D_s\,V_m\,k_f} + \frac{V_s^2}{V_m^2\,k_f^2}\right)$$

$$+ \left(\frac{L}{U} + \frac{2D}{U^2}\right) k' \left(\frac{136\,d_f^6}{105\,D_s^3} + \frac{136}{15} \cdot \frac{d_f^4}{D_s^2} \cdot \frac{V_s}{V_m\,k_f} + 24 \cdot \frac{d_f^2}{D_s} \cdot \frac{V_s^2}{V_m^2\,k_f^2} + 24 \cdot \frac{V_s^3}{V_m^3\,k_f^3}\right)$$

* The effect of gas phase compressibility on the exact value of the moments is neglected.

From the expressions derived in gas–liquid chromatography[6] and given in Table I, neglecting the higher-order terms in D^2/U^4 in the second moment equation, it is possible to derive the theoretical plate height:

$$H = L \cdot \frac{m_2}{m_1'^2} \tag{9}$$

where L is the column length, and thus

$$H = \frac{2D}{U} + \frac{2\,k'}{(1+k')^2} \cdot \frac{d_f^2}{3D_s} \cdot U \tag{10}$$

or

$$H = \frac{2D}{U} + C_l\,U \tag{11}$$

where C_l accounts for the resistance to mass transfer in the liquid phase, neglecting the mass transfer across the mobile–stationary phase interface[14].

The third moment is usually expressed relative to the third power of the standard deviation (skew coefficient). However, Grubner[5] has shown that a simple expression relates the specific asymmetry ($m_3/m_1'^3$) to the carrier gas velocity.

Using the same assumptions as for the derivation of H, we can derive from the expression of the third moment in gas–liquid chromatography (*cf.*, Table I and ref. 6):

$$Z = \frac{m_3}{m_1'^3} \cdot L^2 = \frac{12D^2}{U^2} + \frac{12D\,k'}{(1+k')^2} \cdot \frac{d_f^2}{3D_s} + \frac{12\,k'}{(1+k')^3} \cdot \frac{d_f^4}{15D_s^2} \cdot U^2 \tag{12}$$

or, using eqns. 10 and 11:

$$Z = \frac{12D^2}{U^2} + 6D\,C_l + \frac{9}{5}\left(\frac{1+k'}{k'}\right) C_l^2\,U^2 \tag{13}$$

The specific excess can be derived similarly:

$$F = \frac{m_4}{m_1'^4} \cdot L^2 = \frac{12D^2}{U^2} + 24D \cdot \frac{k'}{(1+k')^2} \cdot \frac{d_f^2}{3D_s} + 12 \cdot \frac{k'^2}{(1+k')^4} \cdot \frac{d_f^4}{9D_s^2} \cdot U^2 +$$

$$+ \frac{k'}{(1+k')^3} \cdot \frac{96D}{15} \cdot \frac{d_f^4}{D_s^2} \cdot \frac{U}{L} + \frac{k'}{(1+k')^4} \cdot \frac{136}{105} \cdot \frac{d_f^6}{D_s^3} \cdot \frac{U^3}{L} \tag{14}$$

The last two terms in eqn. 14 are negligible if the column is long enough, and thus

$$F = \frac{m_4}{m_1'^4} \cdot L^2 = 3H^2 = \frac{12D^2}{U^2} + 12D\,C_l + 3C_l^2\,U^2 \tag{15}$$

This very simple relationship could not be derived by Grubner[5] in his discussion on the statistical moments in gas–solid chromatography as the second and the third terms of the fourth moment expression he gave are erroneous, as well as those given in the original work of Kucera[4]. The correct expression of the fourth moment in gas–solid chromatography can be derived by analogy with the one given in Table I for gas–liquid chromatography.

Eqn. 15 shows that it is not necessary to measure the fourth moment in order to study fast exchange processes in a chromatographic column, as no new information can be derived from it. This just means that the theory of linear chromatography with finite kinetics predicts that the excess value, E, is 3, the value obtained for a gaussian shape profile, even if the peak is not symmetrical.

The expressions of statistical moments derived in gas–solid chromatography or in gas–liquid chromatography account for the molecular and the apparent diffusion processes inside the column, as well as the resistance to mass transfer, assuming fast exchange reactions on one type of site. This picture is very approximate, especially in gas–solid chromatography, as adsorbents have a wide pore size distribution. Even with the fairly homogeneous, non-porous surface of graphitized thermal carbon black, active sites, generally functional groups or impurities, exist which have not been eliminated by the thermal treatment. They are not considered in the moment theory.

In gas–liquid chromatography, the stationary phase is distributed in a complex geometrical way, probably with a wide range of structures incorporating areas on which films of very different thickness are coated and droplets of various sizes. It cannot therefore be assumed that something like a constant film thickness does exist. A rigorous way of solving this problem in linear chromatography is the stochastic approach of Giddings and Eyring[2] and McQuarrie[3] for studying peak profiles.

RESULTS AND DISCUSSION

In the first section below we discuss the choice of a model to account for the peak profile in different experimental conditions. The physical significance of the results obtained is discussed in the second part.

1. Chromatographic profiles

Concentration profile of fast exchange processes. The elution peak of *n*-pentane on the highly loaded squalane column is almost symmetrical and a very good fit of the experimental data with the Gram–Charlier series is observed.

In Fig. 1a is represented a typical chromatogram in reduced coordinates, so that the total surface area under the distribution curve, $P(\theta)$, is 1 with $\theta = (t - t_{max})/t_m$. The points are the experimental data collected by the computer, while the line is calculated from the Gram–Charlier series expanded to the fourth Hermite polynomial (eqn. 6). Accordingly, five constants are sufficient to characterize completely this peak profile: the peak area (m_0), its mass centre (m'_1), the standard deviation (σ), the skew coefficient ($S = A_3$) and the excess ($E = A_4 + 3$).

The standard deviation, the skew coefficient and the excess calculated from the least-squares fit of the Gram–Charlier series on the experimental data in Fig. 1a are $\sigma^2 = 55.92\ \text{sec}^2$, $S = 0.16$ and $E = 3.07$, while the corresponding values cal-

culated from the moments obtained by numerical integration of the same experimental data are $\sigma^2 = 57.71$ sec^2, $S = 0.25$ and $E = 3.49$. The differences are very significant, about six times the standard deviation of the error on the direct calculation of S and E. Furthermore, when these last values are introduced into the Gram–Charlier series to account for the peak profile, the curve obtained is distorted (Fig. 1b) and

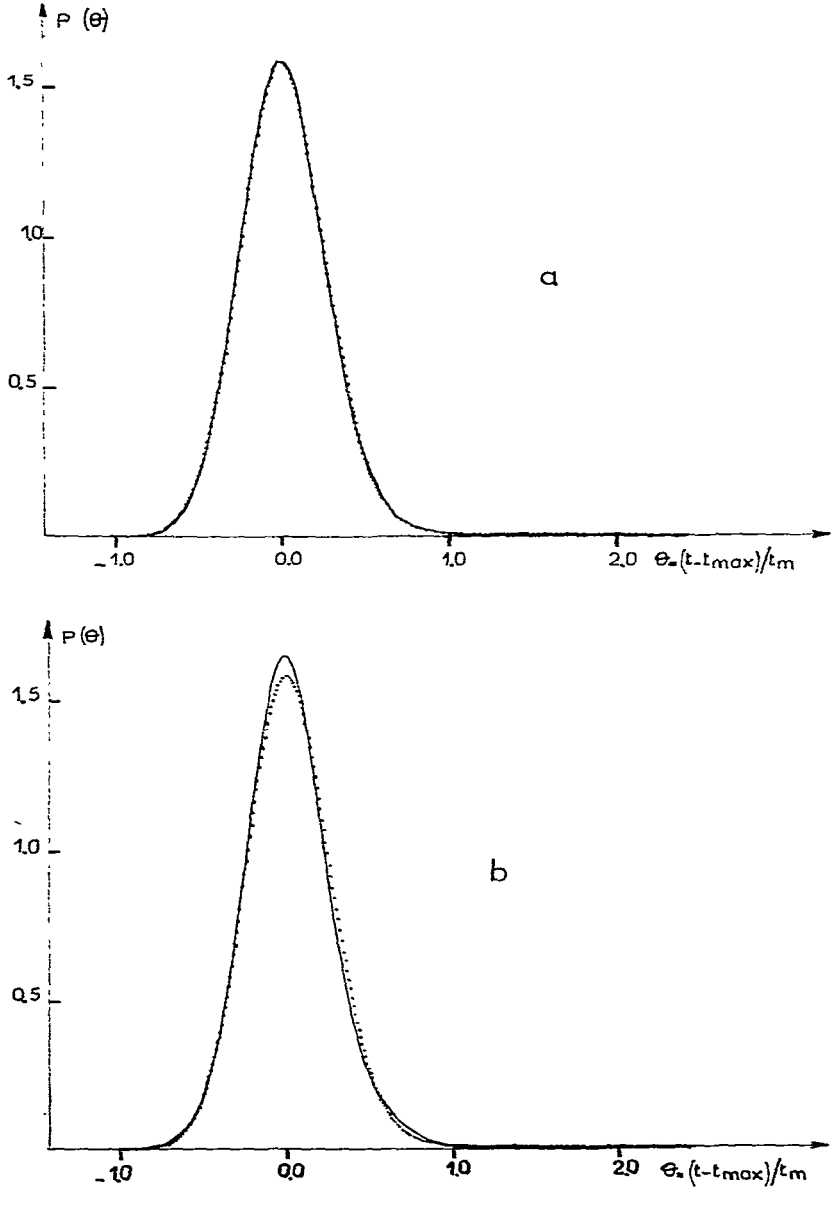

Fig. 1.

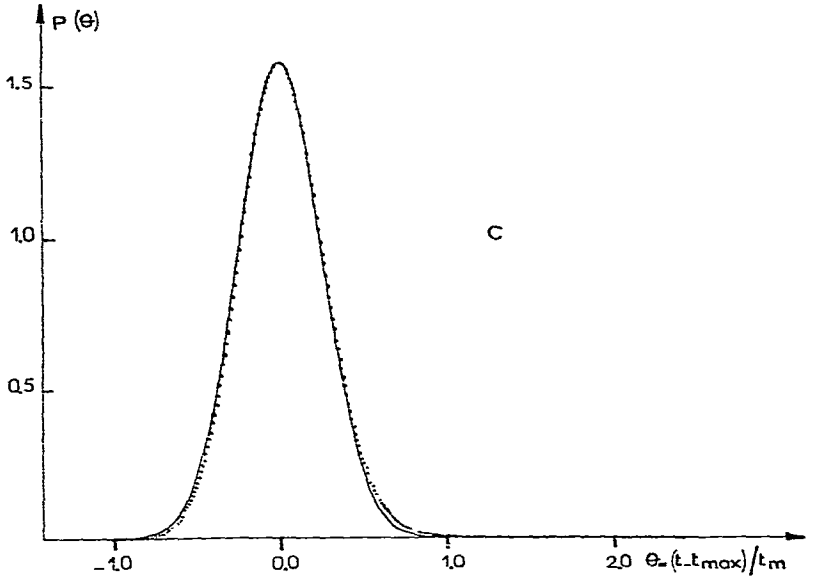

Fig. 1. Elution profile of *n*-pentane on a 2-m column packed with 20% squalane on Chromosorb P. Temperature, 50°; carrier gas, helium; pressure drop, 1800 mbar; flow-rate, 14.4 cm³/min; sample size, 3.1 μg; unretained peak retention time, $t_m = 29.37$ sec. Points, digitalized data of the chromatogram; solid line, theoretical model. (a) Best Gram–Charlier theoretical model obtained by least-squares fit on the experimental data; $m_0 = 95062$; $m_1' = 359.04$ sec; $m_2 = \sigma^2 = 55.92$ sec²; $S = 0.16$; $E = 3.07$. (b) Gram–Charlier series using the moments obtained by integration: $m_0 = 95240$; $m_1' = 359.03$ sec; $m_2 = \sigma^2 = 57.71$ sec²; $S = 0.25$; $E = 3.49$. (c) Best Poisson theoretical model obtained by curve fitting: $m_1' = 358.85$; $N = 2349$.

does not represent the peak profile as well as the "best" Gram–Charlier series. Perhaps it represents the tail better, and this would be a good illustration of the ambiguity of peak profile analysis, namely to decide what is the most important part of the profile, the main peak or its tail.

To visualize the high degree of symmetry of the *n*-pentane peak (Fig. 1c), a Poisson-law model, which is the correct model for an ideal chromatographic profile[9] and is almost identical with a gaussian profile in the case in point, is fitted to the experimental data. The equation of the profile if $N > 10$ is

$$f(t) = \frac{m_0}{\sqrt{2\pi(N-1)}} \cdot \left(\frac{t}{m_1'}\right)^{N-1} \cdot \frac{N^N}{(N-1)^{N-1}} \cdot \exp\left[-N\left(\frac{t}{m_1'}\right) + N - 1\right] \qquad (16)$$

where N is the plate number (2349). This gives the values $\sigma^2 = 54.82$ sec², $S = 0.04$ and $E = 3.003$.

In Table II are given the skew, the excess, the specific asymmetry and excess multiplied by L^2 (Z and F coefficients, *cf.* eqns. 12 and 14) as a function of the flow velocity for *n*-pentane at 50° with helium as the carrier gas. The standard deviation of the error of the measurement of these parameters, calculated from the dispersion of the data for various injections of *n*-pentane at the same pressure (generally six) is

TABLE II

COMPARISON BETWEEN SKEW AND EXCESS, DERIVED FROM DIRECT NUMERICAL INTEGRATION AND FROM LEAST-SQUARES FIT OF THE GRAM-CHARLIER SERIES

Solute *n*-pentane. Column packed with 20% squalane on Chromosorb P at 50°. Carrier gas, helium.

ΔP (mbar)	$\bar{u}$ (cm/sec)	Moments calculated by numerical integration				Moments calculated from Gram-Charlier least-squares fit			
		S	E	Z (cm²)	F (cm²)	S	E	Z (cm²)	F (cm²)
600	2.404	0.111	3.038	0.076	0.053	0.104	3.003	0.067	0.052
		$\sigma = 0.008$	$\sigma = 0.007$	$\sigma = 0.001$	$\sigma = 0.001$	$\sigma = 0.013$	$\sigma = 0.007$	$\sigma = 0.009$	$\sigma = 0.001$
1000	3.913	0.187	3.327	0.077	0.030	0.124	3.035	0.049	0.026
		$\sigma = 0.004$	$\sigma = 0.015$	$\sigma = 0.001$	$\sigma = 0.002$	$\sigma = 0.002$	$\sigma = 0.006$	$\sigma = 0.001$	$\sigma = 0.001$
1400	5.360	0.236	3.473	0.085	0.026	0.147	3.057	0.051	0.022
		$\sigma = 0.005$	$\sigma = 0.017$	$\sigma = 0.002$	$\sigma = 0.002$	$\sigma = 0.002$	$\sigma = 0.003$	$\sigma = 0.001$	$\sigma = 0.001$
1800	6.767	0.275	3.583	0.105	0.029	0.167	3.069	0.060	0.023
		$\sigma = 0.016$	$\sigma = 0.083$	$\sigma = 0.007$	$\sigma = 0.001$	$\sigma = 0.005$	$\sigma = 0.005$	$\sigma = 0.002$	$\sigma = 0.001$
2200	8.128	0.299	3.961	0.134	0.040	0.187	3.087	0.077	0.028
		$\sigma = 0.082$	$\sigma = 0.385$	$\sigma = 0.035$	$\sigma = 0.005$	$\sigma = 0.013$	$\sigma = 0.023$	$\sigma = 0.006$	$\sigma = 0.001$
2600	9.457	0.341	3.826	0.178	0.047	0.188	3.078	0.091	0.034
		$\sigma = 0.002$	$\sigma = 0.016$	$\sigma = 0.001$	$\sigma = 0.001$	$\sigma = 0.003$	$\sigma = 0.005$	$\sigma = 0.001$	$\sigma = 0.001$

also given. The very good reproducibility of all peak profile parameters can be seen. The moments calculated by numerical integration are known to within about 10% at the 95% confidence level, while those derived from the Gram–Charlier fit are known to within less than 5%.

In fact, large systematic errors appear in the derivation of the moments obtained by numerical integration. These errors occur mainly from the limits of integration which are too narrow, but cannot be made wider for other reasons[8], the baseline drift, the noise of the signal and the possible occurrence of impurities in the solute. Although the experimental conditions selected for this experiment were ideal (signal-to-noise ratio *ca.* 500 at the peak maximum, no baseline drift and solute of high purity), the small tailing increases the second, the third and the fourth statistical moments markedly and the values measured are too large.

This is even more obvious for methane elution peaks (Fig. 2a). In this instance also, the Gram–Charlier series is a good model for the profile and we obtain $\sigma^2 = 0.47$ sec^2, $S = 0.45$ and $E = 3.36$. The corresponding profile is plotted on Fig. 2a and the fit is very good, except on the peak tail.

When the parameters obtained by numerical integration are introduced into the Gram–Charlier series, a completely impossible profile is obtained and large oscillations around the baseline occur (Fig. 2b). Similar oscillations have been reported by Villermaux[9], who was unable to reproduce the elution profiles using the Gram–Charlier series and the experimental values of the moments. This, in fact, is not surprising if one remembers the theoretical background of the Gram–Charlier series[3]. It is an expansion of the normal distribution and can account only for moderately unsymmetrical peaks, not long, low edges at the end of a nearly symmetrical peak, as is the case here.

Probably the small tailing of the methane peak arises from extra-column effects such as diffusion in dead volumes at the column inlet. This increases dramatically the values of the statistical moments, as can be seen in Table III, where the S, E, Z and F coefficients are given for methane with both calculation methods. The high values of the moments obtained by numerical integration result only from the length of the peak tail. Both sets of moments are fairly reproducible, however (*cf.*, Table III), and the chromatographic profiles are reproducible even for their tailing part.

These results show that the Gram–Charlier series appears to be a very good model to account for peak shapes when the tailing is small. In the second part of this discussion we consider the diffusion and mass-transfer processes of *n*-pentane in the highly loaded squalane column using the moments obtained from the least-squares fit of the Gram–Charlier series on the digitalized data of the chromatogram.

Concentration profiles of tailing elution peaks. As shown by Giddings[10], tailing is often not caused by column overloading but by sorption sites which hold molecules for a period as long as that needed to elute one quarter of the zone (*i.e.*, about one time standard deviation) or longer. Two examples of such tailing elution profiles are given here, while a systematic study of these profiles as a function of the various experimental parameters, in relation to the statistical moments, will be given in a later paper[15].

Under conditions where the isotherm is linear (retention independent of sample size), a marked degree of tailing was observed for cyclohexane eluted on a column

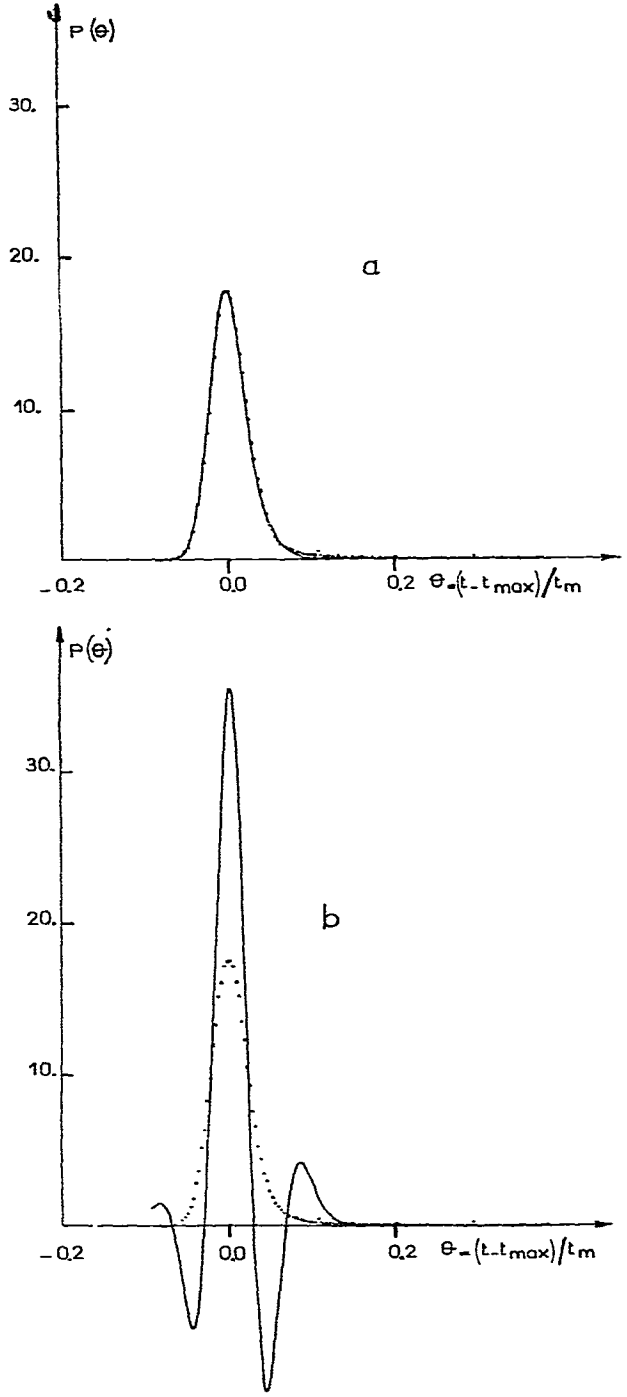

Fig. 2. Elution profile of methane on the same column as for Fig. 1. Amount injected: 0.1 μg. Same experimental conditions as for Fig. 1. (a) Best Gram–Charlier theoretical model obtained by least-squares fit of the experimental data: $m_0 = 2970$; $m_1' = 29.46$ sec; $m_2 = \sigma^2 = 0.47$ sec^2; $S = 0.45$; $E = 3.36$. (b) Gram–Charlier series corresponding to the moments obtained by integration: $m_0 = 3028$; $m_1' = 29.53$ sec; $m_2 = \sigma^2 = 0.77$ sec^2; $S = 2.23$; $E = 15.86$.

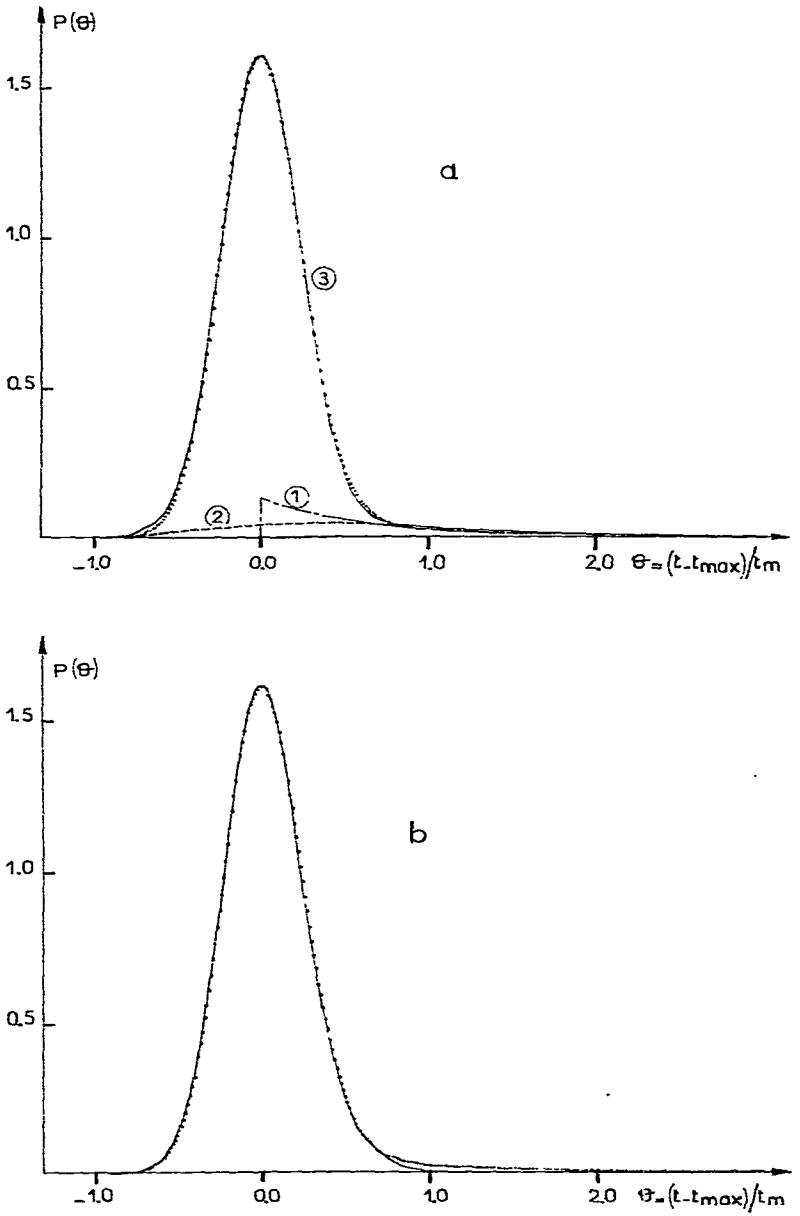

Fig. 3. Elution profile of cyclohexane on a 2-m column packed with porous glass beads coated with 0.5% squalane. Temperature, 30°; carrier gas, helium; pressure drop, 600 mbar; flow-rate, 8.6 cm^3/min; amount injected, $0.54 \cdot 10^{-7}$ g; unretained peak retention time, $t_m = 34.13$ sec. Moments from numerical integration: $m_0 = 39252$; $m_1' = 399.07$ sec; $\sigma^2 = 142.21$ sec^2; $S = 3.01$; $E = 27.60$. Points: digitalized data of the chromatogram. (a) Giddings[10] model for tailing peaks (curve 3). Curve 1 = eqn. 1; curve 2 = diffusion processes applied to curve 1; curve 3 = total theoretical chromatogram = curve 2 + Poisson model. Theoretical model parameters: $m_0 = 39252$; $m_1' = 397.26$ sec; $N = 2463$; $a_1 = 0.080$; $a_2 = 1.40$. (b) Best Gram–Charlier theoretical model by curve fitting: $m_0 = 38371$; $m_1' = 397.95$ sec; $\sigma^2 = 72.96$ sec^2; $S = 0.33$; $E = 3.24$.

TABLE III

COMPARISON BETWEEN SKEW AND EXCESS, DERIVED FROM DIRECT NUMERICAL INTEGRATION AND FROM LEAST-SQUARES FIT OF THE GRAM-CHARLIER SERIES

Sample, methane. Column, packed with 20% squalane on Chromosorb P at 50°. Carrier gas, helium.

ΔP (mbar)	$\bar{u}$ (cm/sec)	*Moments calculated by numerical integration*				*Moments calculated from Gram-Charlier least-squares fit*			
		S	E	Z (cm^2)	F (cm^2)	S	E	Z (cm^2)	F (cm^2)
600	2.404	0.19	3.19	0.39	0.25	0.187	3.042	0.385	0.233
		$\sigma = 0.04$	$\sigma = 0.09$	$\sigma = 0.07$	$\sigma = 0.01$	$\sigma = 0.011$	$\sigma = 0.035$	$\sigma = 0.046$	$\sigma = 0.009$
1000	3.913	0.54	4.37	0.62	0.15	0.304	3.166	0.308	0.094
		$\sigma = 0.04$	$\sigma = 0.25$	$\sigma = 0.06$	$\sigma = 0.01$	$\sigma = 0.004$	$\sigma = 0.004$	$\sigma = 0.004$	$\sigma = 0.004$
1400	5.360	1.34	9.03	1.35	0.27	0.412	3.305	0.277	0.057
		$\sigma = 0.08$	$\sigma = 0.69$	$\sigma = 0.12$	$\sigma = 0.03$	$\sigma = 0.005$	$\sigma = 0.006$	$\sigma = 0.003$	$\sigma = 0.001$
1800	6.767	1.96	13.60	1.92	0.39	0.440	3.395	0.226	0.041
		$\sigma = 0.19$	$\sigma = 1.61$	$\sigma = 0.28$	$\sigma = 0.07$	$\sigma = 0.019$	$\sigma = 0.030$	$\sigma = 0.008$	$\sigma = 0.001$
2200	8.128	2.73	20.69	3.12	0.74	0.498	3.403	0.210	0.032
		$\sigma = 0.59$	$\sigma = 5.91$	$\sigma = 1.45$	$\sigma = 0.47$	$\sigma = 0.014$	$\sigma = 0.031$	$\sigma = 0.004$	$\sigma = 0.001$
2600	9.457	3.38	27.35	4.13	1.05	0.532	3.446	0.204	0.028
		$\sigma = 0.19$	$\sigma = 2.30$	$\sigma = 0.50$	$\sigma = 0.18$	$\sigma = 0.005$	$\sigma = 0.008$	$\sigma = 0.002$	$\sigma = 0.004$

packed with porous glass beads coated with a small amount of squalane. To represent the elution profile (Fig. 3a), we used the model proposed by Giddings[10]. The dotted line (1) is a plot of eqn. 1; it is characterized by values of the adsorption and desorption rate constants derived from the curve fitting described below. The second curve is derived from the first by convolution using the Schmidt method[16], as demonstrated by Giddings, to allow for the effective diffusion processes in the column. On this profile (curve 2) is superimposed a Poisson-law model curve which corresponds to the total diffusion processes through the column, applied to the δ-injection profile (*cf.*, eqn. 2).

Three steps are necessary to account for an experimental profile:

(a) adjusting eqn. 1 on the tail of the peak which gives curve 1;

(b) diffusion process of curve 1 into curve 2, using Schmidt method;

(c) subtraction of curve 2 from the numerical data of the chromatogram and adjustment of a Poisson-law model, using a least-squares fit. The resulting model, curve 3, is the sum of the "best" Poisson law and of curve 2.

For the profile shown in Fig. 3a, we have an excellent fit with $a_1 = 0.080$ and $a_2 = 1.40$. As $t_m = 34.13$ sec, the adsorption and desorption rate constants are $k_a = 2.35 \cdot 10^{-3}$ sec^{-1} and $k_d = 40.8 \cdot 10^{-3}$ sec^{-1}. The plate number obtained for the Poisson law representing the molecules which are not adsorbed on the tail producing sites is $N = 2463$; m'_1 represents the retention time of the fast exchange process. For six different injections the standard deviation obtained for a_1 is $\sigma_{a1} = 1.5 \cdot 10^{-3}$ (2%), for a_2, $\sigma_{a2} = 0.06$ (4%), and for N, $\sigma_N = 7$ (0.3%).

The fraction of molecules which are not adsorbed on the strong sites and follow the Poisson model is 0.91. Thus, 9% of the molecules are retained on active sites and the mean time of desorption for these molecules is $\tau_d = 1/k_d$ or 24.5 sec. The tailing is thus caused by active sites for which the desorption time is almost equal to the elution time of an unretained peak and, as can be seen in Fig. 3a, tailing is observed at a distance which corresponds to several times the elution time of a non-retained peak.

Fig. 3b shows the fit of the Gram–Charlier series on the digitalized data of the chromatogram. In this instance, the series is unable to reproduce the tail of the peak but still is a good model for the major part of it. The parameters of the series are $m_2 = \sigma^2 = 72.96$ sec^2, $S = 0.33$ and $E = 3.24$, while those obtained from numerical integration are much larger, $m_2 = 142.21$ sec^2, $S = 3.01$ and $E = 27.60$.

As the major contribution to the moments comes from the tailing part of the peak, the moments cannot give a good picture of the peak which for its largest part (91%) is very sharp, with a σ^2 from the Poisson law of 64.07 sec^2.

The failure of the Gram–Charlier series to represent correctly the long peak tail is due to its character of a derivative of the normal distribution. It can incorporate some degree of asymmetry but not a long, low tail. On the other hand, the Giddings model accounts very well for the peak shapes. Furthermore, it gives valuable information such as the fraction of the molecules which are not adsorbed on active sites and the desorption time from the active sites of the surface.

Fig. 4 shows the peak profile of methylene chloride eluted on the 2-m column packed with 20% squalane on Chromosorb P. The sorption isotherm was almost linear as we observed little change in retention time and peak shape (see ref. 15) when the sample size was changed from 0.1 to 2 μg. With the theoretical model

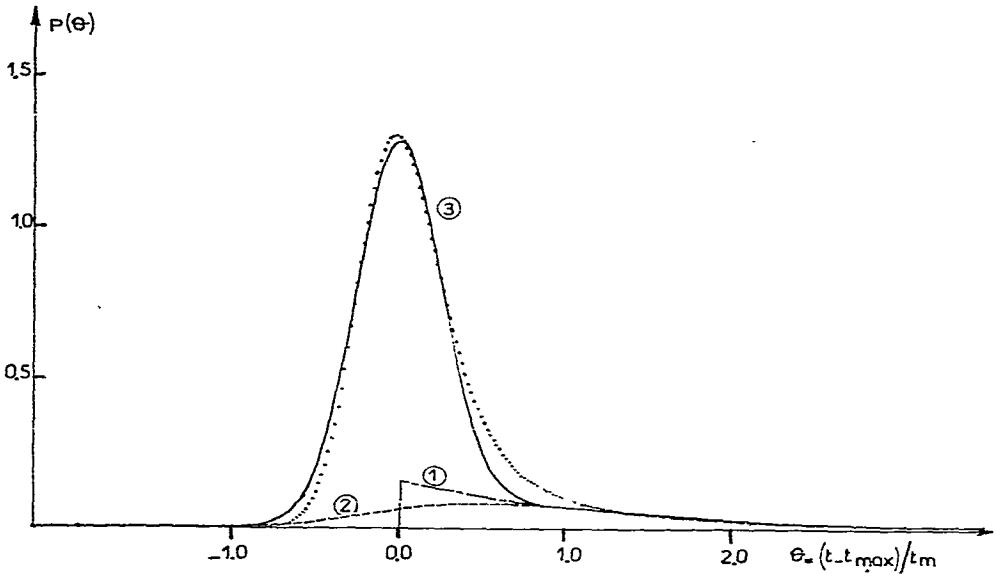

Fig. 4. Elution profile of methylene chloride on the same column as for Fig. 1. Temperature, 50°; carrier gas, helium; pressure drop, 2600 mbar; amount injected, 1.9 μg; unretained peak retention time, $t_m = 20.95$ sec. Moments from numerical integration: $m_0 = 53452$; $m_1' = 225.74$ sec; $\sigma^2 = 220.16$ sec^2; $S = 3.68$; $E = 27.17$. Points: digitalized data of the chromatogram. Giddings[10] model for tailing (curve 3). Curve 1 = eqn. 1; curve 2 = diffusion processes applied to curve 1; curve 3 = curve 2 + Poisson model. Theoretical model parameters: $m_0 = 53452$; $m_1' = 220.50$ sec; $N = 1623$; $a_1 = 0.21$; $a_2 = 0.98$.

assumed, molecules of methylene chloride are held on active sites, probably those of the support surface, for a long time. When desorption finally occurs, the bulk of the zone (81% with $a_1 = 0.21$) has already passed. The desorption time from the active sites, $\tau_d = t_m/a_2$, is 21.4 sec. The model is again a good representation of the chromatographic peaks, considering the simplifications made: a linear sorption isotherm, and only two different types of sites, one with a fast exchange process (the squalane stationary phase) and the other with a long desorption time (active sites of the support). Both assumptions are approximate as more than one type of site exists on the surface of Chromosorb P that may retain methylene chloride, which is a polar compound, for a long period of time; each type of adsorption site has an energy and a residence time distribution and the sorption isotherm of methylene chloride on the support itself is not linear.

For both profiles (Figs. 3 and 4), the time constant of the exponential adjusted on the tail of the peak[8] is a good estimate of the desorption time from the active sites. This is because at high values of time, $P_1(\theta)$ behaves as $e^{-a_2\theta}$. For cyclohexane, the desorption time is 24.5 sec and the time constant of the exponential is 21.0 sec, while for methylene chloride the desorption time is 21.4 sec and the time constant of the exponential is 31.3 sec. It is thus theoretically justified to adjust an exponential on the tail of non-symmetrical peaks, in order to avoid the systematic error in the numerical integration during calculation of the central moments which arises from the finite width of the integration limits.

II. Study of column diffusion processes

The column diffusion processes and resistances to mass transfer were studied through the statistical moment approach for *n*-pentane and methane, on the column packed with 20% squalane on Chromosorb P. The moments derived from the Gram–Charlier least-squares fit are compared to the moments obtained by integration.

First statistical moment. The first moments are identical, within the errors of measurement.

Second central statistical moment. The second central moment can conveniently be studied as a function of the carrier gas velocity, U, using the HETP definition: $H = Lm_2/m_1'^2$ (eqn. 9).

For *n*-pentane, a good model of the relationship between H and U is given by the equation recommended by Giddings and Schettler[17] for gas–liquid chromatography:

$$\frac{H}{f} = \frac{B}{u_s} + C_g u_s + C_l \bar{u} \tag{17}$$

where u_s is the outlet gas velocity and $\bar{u}$ the main velocity with $u_s = \bar{u}/j$ and C_g the coefficient for resistance to mass transfer term in the gaseous phase; j and f are pressure correction terms considering the volume expansion of the gas phase and the change of the diffusion coefficient with the pressure:

$$j = \frac{3}{2} \cdot \frac{(P^2 - 1)}{(P^3 - 1)} \tag{18a}$$

and

$$f = \frac{9}{8} \cdot \frac{(P^4 - 1)(P^2 - 1)}{(P^3 - 1)^2} \tag{18b}$$

with $P = P_i/P_0$ where P_i is the inlet pressure and P_0 the outlet pressure. f is very close to 1 in the pressure range studied and as the error made in the coefficients in equating f to 1 is less than the experimental error, eqn. 17 can be written as

$$H = \frac{B}{u_s} + C_g u_s + C_l \bar{u} \tag{19}$$

As B is proportional to the diffusion coefficient of the solute in the gas phase at the outlet pressure, $B = 2\gamma D_g$, we have

$$H = \frac{2\gamma D_g}{u_s} + C_g u_s + C_l \bar{u} \tag{20}$$

where γ is the tortuosity factor, which depends on the column packing[1].

Fig. 5 shows a plot of H *versus* u_s/D_g. Such a plot allows a comparison between the experimental data obtained for two different carrier gases, helium and hydrogen, at two different temperatures. The second moments used to calculate the values of H plotted here were derived from the parameters of the Gram–Charlier least-squares fit.

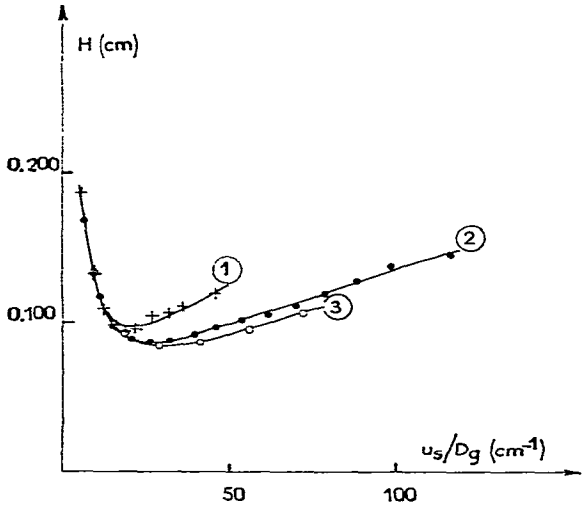

Fig. 5. Plot of H *versus* u_s/D_g, where u_s = carrier gas velocity and D_g = diffusion coefficient of solute in the carrier gas. Solute: *n*-pentane on the same column as for Fig. 1. Carrier gas: 1, hydrogen at 30.1°; 2, helium at 30.1°; 3, helium at 50°.

A smaller column efficiency is observed when hydrogen is used as the carrier gas because, at high gas velocities, the mass transfer term in the liquid stationary phase, $C_l\,\bar{u}$, is predominant. At low carrier gas velocities, the curves coincide as the first term, accounting for longitudinal diffusion, is the major contribution to H.

The coefficients in eqn. 19 are calculated using a linear least-squares fit program, computing also the confidence interval for the coefficients, using the method described by Linnik[18].

In Table IV, we compare the coefficients of eqn. 20 obtained from the second moment calculated by numerical integration, using eqn. 3, with those derived by fitting the Gram–Charlier series to the digitalized data collected by the computer, using a non-linear least-squares fit program.

The diffusion coefficient of the solute in the gaseous phase was calculated using the method of Fuller *et al.*[19].

The second central moments calculated by either method are generally very close, and sometimes slightly higher when calculated by integration. The relative error of the second moment determination is about 1% when calculated by integration and 0.5% when derived from a Gram–Charlier fit on the experimental data. The coefficients in eqn. 19 or 20 giving H as a function of the carrier gas velocity are obtained with an error with the Gram–Charlier fit that is half that with direct integration.

Fig. 6 shows H as a function of the carrier gas velocity for methane at 30.1° with helium as carrier gas. Each experimental point is the mean value of at least six different experiments at the same velocity. The open circles represent the second moment calculated by integration. They are best fitted (*cf.*, broken curve) by the equation

$$H = \frac{B}{u_s} + C_g\,u_s + A \qquad (21)$$

TABLE IV

COMPARISON BETWEEN THE COEFFICIENTS OF THE HETP EQUATION (EQN. 19) OBTAINED FROM THE SECOND CENTRAL MOMENTS CALCULATED BY INTEGRATION AND BY GRAM–CHARLIER FIT

Column: 20% squalane on Chromosorb P, length 2 m.

Experimental conditions	D_g *(cm²/sec)*	*Second central moments*	
		Calculated from numerical integration	*Calculated from Gram–Charlier series*
n-Pentane, He, 30.1°	0.298	$B = 0.30 \pm 0.06$ cm²/sec	$B = 0.30 \pm 0.0$ cm²/sec
$k' = 19.9$		$\gamma = 0.51 \pm 0.10$	$\gamma = 0.50 \pm 0.05$
		$C_g = (1.1 \pm 0.3) \cdot 10^{-3}$ sec	$C_g = (1.2 \pm 0.1) \cdot 10^{-3}$ sec
		$C_l = (8.6 \pm 0.7) \cdot 10^{-3}$ sec	$C_l = (8.1 \pm 0.4) \cdot 10^{-3}$ sec
n-Pentane, He, 50°	0.333	$B = 0.35 \pm 0.08$ cm²/sec	$B = 0.36 \pm 0.06$ cm²/sec
$k' = 11.2$		$\gamma = 0.53 \pm 0.12$	$\gamma = 0.54 \pm 0.09$
		$C_g = (1.0 \pm 0.5) \cdot 10^{-3}$ sec	$C_g = (1.1 \pm 0.2) \cdot 10^{-3}$ sec
		$C_l = (7.6 \pm 1.2) \cdot 10^{-3}$ sec	$C_l = (6.9 \pm 0.5) \cdot 10^{-3}$ sec
n-Pentane, H_2, 30.1°	0.356	$B = 0.33 \pm 0.03$ cm²/sec	$B = 0.34 \pm 0.01$ cm²/sec
$k' = 19.6$		$\gamma = 0.47 \pm 0.04$	$\gamma = 0.47 \pm 0.01$
		$C_g = (7.5 \pm 0.7) \cdot 10^{-3}$ sec	$C_g = (2.7 \pm 3.0) \cdot 10^{-3}$ sec
		$C_l = (0.4 \pm 10) \cdot 10^{-3}$ sec	$C_l = (5.5 \pm 5) \cdot 10^{-3}$ sec

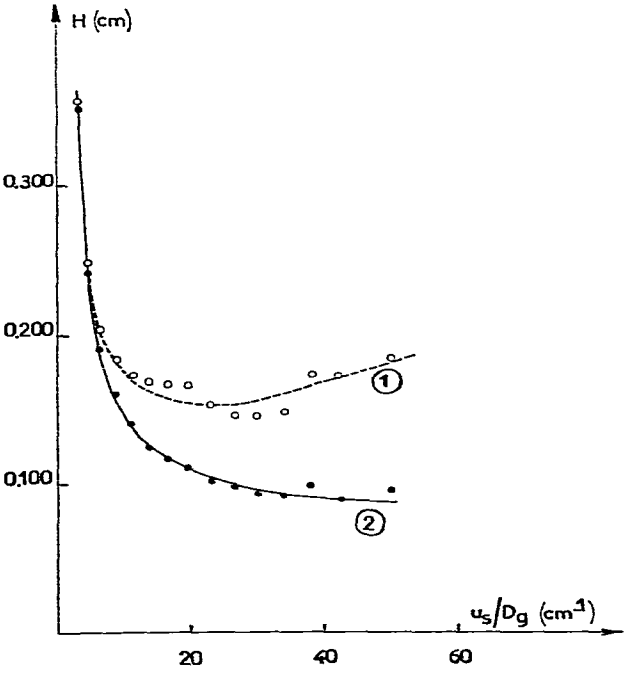

Fig. 6. Plot of *H versus* the carrier gas velocity for methane on the same column as for Fig. 1. Carrier gas: helium at 30.1°. Second central moment calculated either by numerical integration (○, curve 1), or from a least-squares fit of the Gram–Charlier series (●, curve 2).

with $B = 0.53 \pm 0.05$ cm²/sec, $C_g = (1.9 \pm 0.6) \cdot 10^{-3}$ sec and $A = 0.081 \pm 0.016$ cm. As $D_g = 0.695$ cm²/sec, $\gamma = 0.38 \pm 0.04$. The closed circles represents the values of H calculated from the Gram–Charlier fit of the chromatogram, which are best represented by the equation

$$H = \frac{B}{u_s} + A \tag{22}$$

with $B = 0.56 \pm 0.02$ cm²/sec ($\gamma = 0.40 \pm 0.02$) and $A = 0.070 \pm 0.003$ cm.

The use of a coupling term[1] would probably be more accurate than that of a constant term, but the complexity involved at that level of accuracy is not warranted.

The second central moment and the HETP calculated from the parameters of the Gram–Charlier fit are much smaller than those derived through integration of the signal, as the contribution of the tail to the second central moment (see the typical chromatogram in Fig. 2a) is not taken into account in the former instance. The deviation increases with increasing gas velocity, which corresponds to the fact that the C_g term corresponding to curve 2 in Fig. 6 (eqn. 21) is almost negligible, while it is about 2 msec for curve 1. The values of the other two parameters, A and B, are the same. The origin of this rather large C_g term probably lies in a significant contribution of extra-column effects, probably from dead volumes of the instrument at the column inlet.

Third central statistical moment. The third central moment is usually reported to the third power of the standard deviation or the power 3/2 of the second central moment. This parameter is the skew coefficient and is equal to the constant A_3 in the Gram–Charlier series (*cf.*, eqn. 7). This expression does not lead to clear mathematical relationships, however, as shown by Grubner[5], who introduced the asymmetry coefficient, $Z = m_3 L^2 / m_1'^3$, analogous to the HETP.

For *n*-pentane eluted on the column packed with 20% squalane on Chromosorb P, the term for resistance to mass transfer in the liquid phase is large. If we neglect the contribution of resistance to mass transfer in the gas phase, the relationship between H and U (eqn. 11) derived by Grushka[6] for gas–liquid chromatography is valid and eqns. 12 and 13 relating Z and U can thus be used to describe our system. However, these equations do not take into account the effect of the pressure drop across the column. By analogy with the H equation (compare eqns. 11 and 20) with $D = \gamma D_g$, we can write

$$Z = \frac{12\,\gamma^2 D_g^2}{u_s^2} + 6\,\gamma\,D_g\,C_l + \frac{9}{5}\left(\frac{1 + k'}{k'}\right) C_l^2\,\bar{u}^2 \tag{23}$$

or

$$Z = \frac{B'}{u_s^2} + A' + C'\,\bar{u}^2 \tag{24}$$

with

$$A' = 3B\,C_l;\; B' = 3\,B^2;\; C' = \frac{9}{5}\left(\frac{1 + k'}{k'}\right) C_l^2 \tag{25}$$

Fig. 7a shows the variation of Z, the specific asymmetry multiplied by L^2, with the carrier gas velocity. The qualitative agreement with the dependence described by eqn. 24 is excellent. The third moments used for Fig. 7a are derived from the parameters of the best Gram–Charlier fit on the elution profiles. In this figure are reported the parameters derived from the three series of experiments carried out with *n*-pentane on the 2-m column packed with 20% squalane on Chromosorb P: at 30.1° and 50° with helium as carrier gas and at 30.1° with hydrogen as carrier gas. For one of the curves only, for the sake of clarity, the precision of the data is also reported.

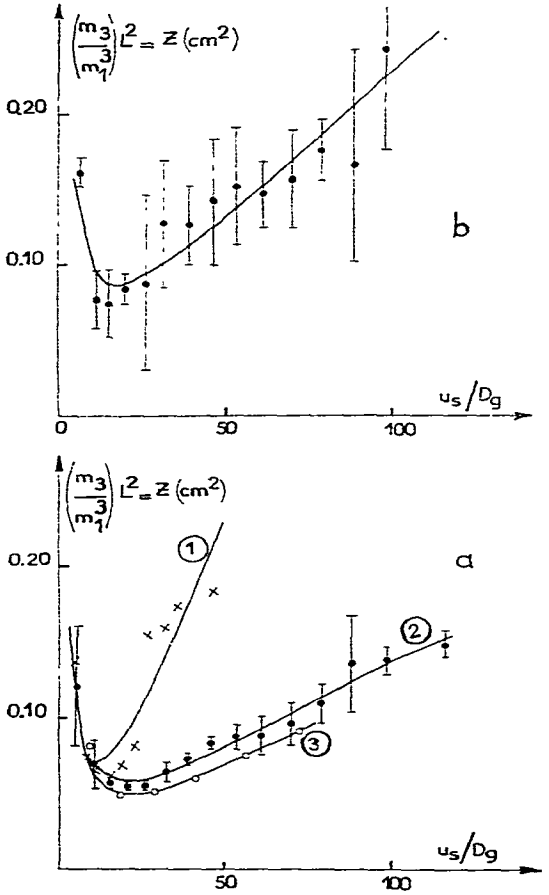

Fig. 7. Plot of Z (eqn. 24) *versus* the carrier gas velocity for *n*-pentane on the same column as for Fig. 1. (a) Third moment from least-squares fit of the Gram–Charlier series. Carrier gas: 1, hydrogen at 30.1°; 2, helium at 30.1°; 3, helium at 50°. (b) Third moment calculated by numerical integration. Carrier gas: helium at 30.1°. The vertical segments have a length equal to 4 times the standard deviation of the measurement.

Table V summarizes the coefficients of eqn. 24 derived for the different experiments by a least-squares fit of the data plotted in Fig. 7. The B' term obtained is in good agreement with that derived from the HETP equation as well as the tortuosity factor derived from it (*cf.*, Table IV).

TABLE V

COMPARISON BETWEEN THE COEFFICIENTS OF Z (EQUATION 24) OBTAINED FROM THE THIRD CENTRAL MOMENT CALCULATED BY INTEGRATION AND BY THE LEAST-SQUARES FIT OF THE GRAM–CHARLIER SERIES

Column: 20% squalane on Chromosorb P, length 2 m.

Experimental conditions	D_g *(cm²/sec)*	*Third central moments*	
		Calculated from numerical integration	*Calculated from Gram–Charlier series*
n-Pentane, He, 30.1° $k' = 19.9$	0.298	$B' = 0.36 \pm 0.19\,cm^4/sec^2$ $\gamma = 0.58 \pm 0.18$ $A' = 0.055 \pm 0.023\,cm^2$ $C' = (13.6 \pm 2.8)\cdot 10^{-4}\,sec^2$	$B' = 0.33 \pm 0.05\,cm^4/sec^2$ $\gamma = 0.56 \pm 0.04$ $A' = 0.033 \pm 0.006\,cm^2$ $C' = (8.3 \pm 0.7)\cdot 10^{-4}\,sec^2$
n-Pentane, He, 50° $k' = 11.2$	0.333	$B' = 0.60 \pm 0.20\,cm^4/sec^2$ $\gamma = 0.67 \pm 0.16$ $A' = 0.041 \pm 0.015$ $C' = (14.8 \pm 2.4)\cdot 10^{-4}\,sec^2$	$B' = 0.55 \pm 0.05\,cm^4/sec^2$ $\gamma = 0.64 \pm 0.04$ $A' = 0.023 \pm 0.004\,cm^2$ $C' = (7.6 \pm 0.6)\cdot 10^{-4}\,sec^2$
n-Pentane, H_2, 30.1° $k' = 19.6$	0.356	Too large errors are made in the determination of the third moments	$B' = 0.40 \pm 0.02\,cm^4/sec^2$ $\gamma = 0.51 \pm 0.02$ $A' = 0.025 \pm 0.036\,cm^2$ $C' = (17.7 \pm 0.6)\cdot 10^{-4}\,sec^2$

The C' term, on the other hand, is about seven times larger than that predicted by theory (*cf.*, eqns. 13 and 23–25) from the HETP equation. For *n*-pentane at 30.1° with helium as carrier gas, C_l as obtained from the plate-height equation is $8.1\cdot 10^{-3}$ sec (Table IV). This results in a calculated value of $1.24\cdot 10^{-4}$ sec² for C' instead of $8.3\cdot 10^{-4}$ sec² as measured (*cf.*, Table V). Alternatively, using the value of C' as measured to predict C_l gives $21\cdot 10^{-3}$ sec. Similarly at 50° C_l is $7\cdot 10^{-3}$ sec from the plate-height equation instead of $20\cdot 10^{-3}$ sec from the Z equation.

The A' coefficient can be derived from the values of γ and C_l as calculated from C' in the Z equation (*cf.*, eqns. 24 and 25). From the values of C' and γ in Table V we obtain $A' = 0.021$ cm² at 30.1° and $A' = 0.026$ cm² at 50°. These values are in very good agreement in all instances with the A' coefficients determined from the Z equation with the linear least-squares fit. On the other hand, if we derive the C_l values from the constant A' term in eqn. 24 and reported in Table V, we find values which are 5–7 times larger than the values of C_l from the HETP equation.

The relationship between Z and the carrier gas velocity is thus very well represented by eqns. 24 and 25, although the C_l term is larger than that predicted from the HETP equation. This increased asymmetry at large carrier gas velocities can be caused by larger diffusion times through some large pools of liquid stationary phase which are prone to exist as the amount of squalane on Chromosorb P is important and the liquid does not spread uniformly over the whole support surface. Therefore, the thickness of the stationary film is not constant and the theory described by the eqns in Table I is only an approximation. The asymmetry, larger than that predicted by the theory deriving the moments from the mass-balance equation at high carrier gas velocities, may have the same kinetic origin as that described by Giddings[10] to explain tailing in gas–liquid chromatography, where a small percentage of the stationary liquid phase is located in pores in which the solute may diffuse for a time longer than average.

We consider that this asymmetry cannot arise from extra-column effects as the column capacity factor is very large ($k' = 19.9$ at 30.1°) and the contribution of extra-column effects decreases as $(1 + k')^{-2}$. The isotherm is linear as we have checked that the column capacity factor does not change within the experimental error made in the determination of the centre of gravity of the profile ($0.5 \cdot 10^{-3}$) when the sample size is increased from 0.01 to 10 μg.

The C' coefficient is about twice as great with hydrogen as with helium as the carrier gas. The error in the C' values, however, is important as the noise level of the flame-ionization detector increases markedly at large velocities of hydrogen carrier gas, resulting in important errors in the third moment.

The third central moment calculated by integration of the digitalized data is much larger than that from the parameters of the Gram–Charlier fit on the elution profile and the corresponding Z values are scattered, as we have observed large errors for the third moment obtained by numerical integration (*cf.*, Fig. 7b). In Table V, the coefficients of the Z equation (eqn. 24) are reported in order to compare them with those from the Gram–Charlier fit. The values of A' and C' are larger but with more important errors made in their derivation because of the scattering of the Z data.

Our data show that systematic errors as large as 50% can be made in the third moment measured by integration, even with carefully controlled equipment, and even on a peak which is not tailing, and with a signal-to-noise ratio of about 500. Good confidence can be given, on the other hand, to the third moments obtained from the Gram–Charlier fit of the elution profile, as *n*-pentane was represented perfectly by the series (Fig. 1a).

Fig. 8a shows a plot of Z *versus* the carrier gas flow velocity for methane at two different temperatures with helium as the carrier gas. The third central moments used were calculated from the Gram–Charlier least-squares fit.

The data obtained for Z were fitted with the equation

$$Z = \frac{B'}{u^2} + A' \tag{26}$$

with $B' = 1.06 \pm 0.22$ cm^4/sec^2 and $A' = 0.26 \pm 0.02$ cm^2 at 30.1° and $B' = 2.77 \pm 0.50$ cm^4/sec^2 and $A' = 0.22 \pm 0.02$ cm^2 at 50°. Eqn. 26 is consistent with a negligible value of C_l for a non-retained peak. From eqn. 25, however, A' should be zero for a non-retained peak, which is not in agreement with the experimental result. The theory predicts that $B' = 12\,\gamma^2 D_g^2$ (*cf.*, eqn. 12). The corresponding value of γ is 0.43 for the first experiment and 0.62 for the second. Considering the scattering of the data (each point in Fig. 8a is the mean value from at least six experiments), these results are in fairly good agreement with the value obtained from eqn. 22 using H data ($\gamma = 0.40$).

Because of the tailing of the methane peak (*cf.*, chromatogram in Fig. 2a), the values of Z are 10 times larger when calculated by numerical integration and increase rapidly with increasing flow velocity. This is due to the extra-column contribution which is about constant in unit time and increases in relative value when the gas velocity increases and the retention time decreases correspondingly.

Fourth central statistical moment. The fourth central statistical moment is

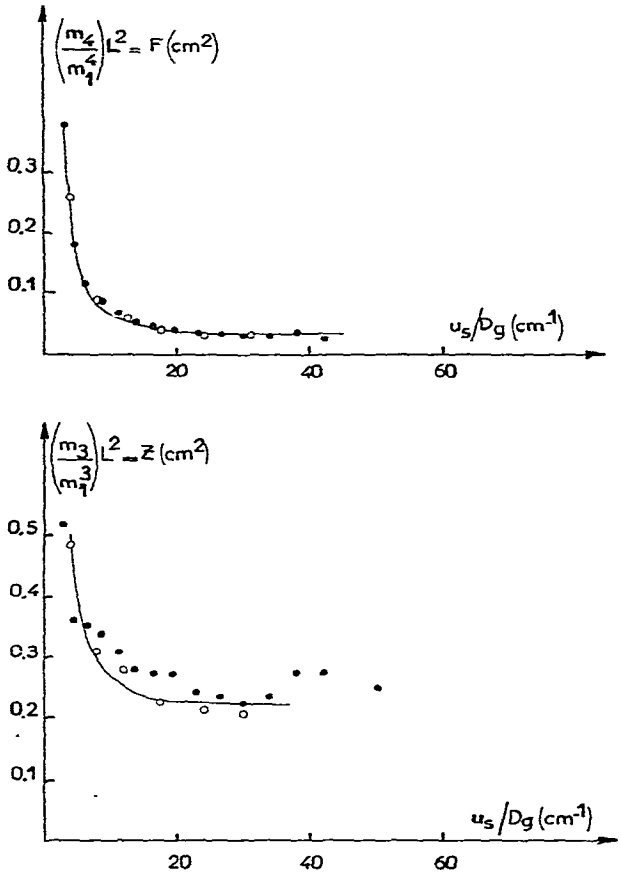

Fig. 8. Plot of Z (eqn. 26) and F (eqn. 27) versus the carrier gas velocity for methane on the same column as for Fig. 1. Carrier gas: ○, helium at 30.1°; ●, helium at 50°.

usually expressed relative to the squares of the second central moment, and this is called the excess. Table II compares the excess values calculated by numerical integration and by least-squares fit of the Gram–Charlier series on the data of the chromatogram collected by the computer for *n*-pentane at 50° with helium as the carrier gas.

The excess is usually very close to 3, the theoretical value for a gaussian peak, when calculated by the second method. This means that the specific excess multiplied by L^2 ($F = m_4L^2/m_1'^4$) is equal to H^2, as predicted from eqn. 15.

The excess values calculated by numerical integration are significantly larger, especially at high velocities (Table II). These values are wrong, however, as the peak shape is perfectly well fitted by the Gram–Charlier series fit ($E = 3.07$ in Fig. 1a) and not by the Gram–Charlier series using the moments calculated by integration ($E = 3.49$ in Fig. 1b). A systematic error occurs when the fourth moment is calculated by integration, which may be as high as 20–30%. This error arises from the fact that the contribution to integration from the tailing edge of the peak is comparatively more important than the major part of the profile.

In Table III, the excess values are given for methane at 50° with helium as the carrier gas. Here again the excess value is much larger when calculated by numerical integration, because of the contribution of tailing to its value (Fig. 2a), and shows a marked increase with increasing velocities. This tailing is due to extra-column effects, as discussed previously.

The change in F as a function of flow velocity was studied using the fourth central moment calculated from the Gram–Charlier least-squares fit. For methane at 30.1° and 50°, with helium as the carrier gas, the specific excess, F, is very well fitted (Fig. 8b) by the equation

$$F = \frac{m_4}{m_1^4} \cdot L^2 = \frac{B''}{u_s^2} + A'' \tag{27}$$

which is in good accordance with the result from eqn. 22 for H, as there is no C_t term for methane, which is not retained on this column. In Fig. 8b each point represents mean value from at least six experiments, and the relative error in F value is less than 5%.

For methane at 30.1°, we have $B'' = 1.38 \pm 0.07$ cm^4/sec^2, $A'' = 0.034 \pm 0.005$ cm^2 and $\gamma = 0.49$. From the B'' coefficient, we derived the tortuosity factor, γ, as $B'' = 12\,\gamma^2 D_g^2$. At 50°, we have $B'' = 2.36 \pm 0.08$ cm^4/sec^2, $A'' = 0.028 \pm 0.003$ cm^2 and $\gamma = 0.57$.

As for the specific asymmetry, good agreement is obtained with the values of the tortuosity factor obtained from the H equation.

A value of A'' significantly different from zero is obtained as in the case of the plot of H *versus* u_s and in the study of the methane peak asymmetry, whereas theory and eqn. 15 predict a zero value, as C_t is negligible. This large value of A'' may come from the extra-column effects which also produce the tailing of the methane peaks (*cf.*, Fig. 2a).

CONCLUSION

The characterization of chromatographic peak profiles by their central statistical moments calculated by direct numerical integration may lead to many errors and uncertainties, even for almost symmetrical elution peaks, which arise from the limits of integration, baseline drift, noise, the presence of small impurities in the solute and extra-column effects, especially in connection with the injection function. Even under the best possible experimental conditions, we have shown that systematic errors occur, which come from the contribution of small tailings at the ends of the peaks.

Curve fitting on the chromatogram collected by the computer leads to more valuable information which cannot be obtained from the moments calculated by numerical integration.

The Gram–Charlier series is a good model for studying the diffusion mechanisms and the rapid exchange processes that take place in the column. Using the values of the central moments calculated from the parameters of the best Gram–Charlier series, we have been able to test the validity of the theories predicting the values of the moments from the mass-balance equation.

The coefficients for longitudinal diffusion obtained from the variation of the second, third and fourth central statistical moments with the gas flow velocity are in good agreement with theory and permit the determination of the tortuosity coefficient when the diffusion coefficient of the solute in the gaseous phase is known.

The higher central statistical moments, even when derived from the Gram–Charlier fit, are very sensitive to small tailings originating from extra-column effects, such as dead volumes or the shape of the injection function. In order to study the rapid exchange processes inside the column itself it is necessary to improve the injection system. The use of fluidic logic systems[20] as sampling devices may help to solve this problem.

Non-symmetrical peaks which have a tail extending for several times the retention time of a non-retained peak are well fitted by the model described by Giddings[10], assuming two types of adsorption sites. From this fit, it is possible to separate the rapid exchange processes from the adsorption on the most active sites of the surface, and to determine the adsorption and desorption rate constants on the tail-producing sites, and the amount of molecules adsorbed on these sites.

Systematic use of these theoretical developments for studying the behaviour of various chromatographic systems is in progress.

ACKNOWLEDGEMENTS

The authors thank Jean-Pierre Olivo for his contribution to the design and construction of the interface between the gas chromatographic instrument and the computer and Guy Thomas for adapting the non-linear least-squares fit programs to the models used.

REFERENCES

1 J. C. Giddings, *Dynamics of Chromatography, Part I: Principles and Theory*, Marcel Dekker, New York, 1965.
2 J. C. Giddings and H. Eyring, *J. Phys. Chem.*, 59 (1955) 416.
3 D. A. McQuarrie, *J. Chem. Phys.*, 38 (1963) 437.
4 E. Kučera, *J. Chromatogr.*, 19 (1965) 237.
5 O. Grubner, *Advan. Chromatogr.*, 6 (1968) 173.
6 E. Grushka, *J. Phys. Chem.*, 76 (1972) 2586.
7 S. N. Chesler and S. P. Cram, *Anal. Chem.*, 43 (1971) 1922.
8 T. Petitclerc and G. Guiochon, *J. Chromatogr. Sci.*, 14 (1976) 531.
9 J. Villermaux, *J. Chromatogr.*, 83 (1973) 205.
10 J. C. Giddings, *Anal. Chem.*, 35 (1963) 1999.
11 J. Villermaux, *J. Chromatogr. Sci.*, 12 (1974) 822.
12 S. D. Mott and E. Grushka, *J. Chromatogr.*, 126 (1976) 191.
13 M. Goedert and G. Guiochon, *Anal. Chem.*, 43 (1971) 1922.
14 M. R. James, J. C. Giddings and H. Eyring, *J. Phys. Chem.*, 68 (1964) 1725.
15 C. Vidal-Madjar and G. Guiochon, in preparation.
16 J. Crank, *The Mathematics of Diffusion*, Clarendon Press, Oxford, 2nd ed., 1975.
17 J. C. Giddings and P. D. Schettler, *Anal. Chem.*, 36 (1964) 1483.
18 Y. V. Linnik, *Methode des Moindres Carrés*, Dunod, Paris, 1963.
19 E. N. Fuller, P. D. Schettler and J. C. Giddings, *Ind. Eng. Chem.*, 58 (1966) 19.
20 G. Gaspar, P. Arpino and G. Guiochon, *J. Chromatogr. Sci.*, in press.